(Received 2 September 2023, Accepted 10 November 2023, Scheduled 20 November 2023)

Enabling Intelligent Metasurfaces for Semi-Known Input

Pujing Lin[1,2,3], Chao Qian[1,2,3*], Jie Zhang[1,2,3], Jieting Chen[1,2,3], Xiaoyue Zhu[1,2,3], Zhedong Wang[1,2,3], Jiangtao Huangfu[1,2,3], and Hongsheng Chen[1,2,3,*]

[1] *ZJU-UIUC Institute, Interdisciplinary Center for Quantum Information State Key Laboratory of Extreme Photonics and Instrumentation Zhejiang University, Hangzhou 310027, China*
[2] *ZJU-Hangzhou Global Science and Technology Innovation Center Key Laboratory of Advanced Micro/Nano Electronic Devices & Smart Systems of Zhejiang Zhejiang University, Hangzhou 310027, China*
[3] *Jinhua Institute of Zhejiang University, Zhejiang University, Jinhua 321099, China*

ABSTRACT: Compelling evidence suggests that the interaction between electromagnetic metasurfaces and deep learning gives rise to the proliferation of intelligent metasurfaces in the past decade. In general, deep learning offers a transformative force to reform the design and working style of metasurfaces. Most of the inverse-design literature announces that, given a user-defined input, pre-trained deep learning models can quickly output the metasurface candidates with high fidelity. However, they largely ignore an important fact, that is, the practical input is always semi-known. In this work, we introduce a generation-elimination network that is robust to semi-known input and information pollution. The network is composed of a generative network to generate a number of possible answers and then a discriminative network to eliminate suboptimal answers. We benchmark the feasibility via two scenes, the on-demand metasurface design of the reflection spectra and the far-field pattern. In the microwave experiment, we fabricated and measured the reconfigurable metasurfaces to automatically meet the semi-known beam steering requirement that widely exist in wireless communication. Our work for the first time answers the question of how to cope with semi-known input, which is ubiquitous in a panoply of real-world applications, such as imaging, sensing, and communication across noisy environment.

1. INTRODUCTION

Probably few people have ever thought about a weird situation in deep learning when we are intoxicated with the intelligent beauty in the past decade, that is, the input of deep learning is semi-known and information-polluted. It implies that part of the information is deterministic, and the rest is undefined and unconcerned. If artificially repairing the undefined part, the output result will be largely contingent on the stochastic repaired version. In the mainstream applications of classification, prediction, translation, and decision, such situation is inconspicuous because it is very straightforward to obtain a fully deterministic input, e.g., video, image, text, and audio [1–3]. However, in other disciplines, such as the burgeoning research on electromagnetic metasurfaces, the situation with semi-known input does exist but remains unanswered.

Metamaterials [4, 5] and their planar version, metasurfaces, have attracted widespread attention in the past decades due to the unparalleled capabilities in manipulating electromagnetic waves and the easy generalization into other physical systems. Realizing versatile capabilities is largely attributed to the high degree of freedom in designing the geometries of constituent unit cell and the spatial arrangement [6–8]. About five years ago, metasurfaces started to gain a lot of traction from the breakthroughs of deep learning [9–13]. As a powerful data-driven method, deep learning allows a computational model to automatically discover many hidden features and then perform tasks without being explicitly programmed and with procedural instructions. The introduction into metamaterials brings many benefits. Among them, accelerating on-demand materials design is an active area of research, exemplified by forward design, inverse design, and spectral correlation [14–17]. Many works have benchmarked that deep learning opens a new pathway to alleviate the time-consuming, experience-guided, and low-efficiency disadvantages in conventional physics-based and full-wave simulations [18–22]. Across various physical scenes, great efforts have been made in improving the design accuracy and reducing data dependency by using novel network structures [23–27].

A universal conclusion drawn in most previous works is that, for an arbitrary given input, the network can output desired metasurface constellations with high accuracy. Indeed, this is important. However, the given input is mostly *artificially constructed*, *purposely-formed*, and actually, *pseudo-arbitrary*. In practice, the input is not easy to be accessed or constructed, rendering it a semi-known problem. When using a widely-used metasurface design to achieve excellent absorption at several resonant frequencies, the construction of the input should be tailored accordingly, without much consideration for other frequencies. Another example is that, if we feed a non-physical electromagnetic response (e.g., the reflection amplitude is larger than unity) into the pre-trained neural network, the output will be certainly wrong; in this case, do we still accept these anomalies or seek for any remedial strategies to cor-

* Corresponding authors: Chao Qian (chaoq@intl.zju.edu.cn); Hongsheng Chen (hansomchen@zju.edu.cn).

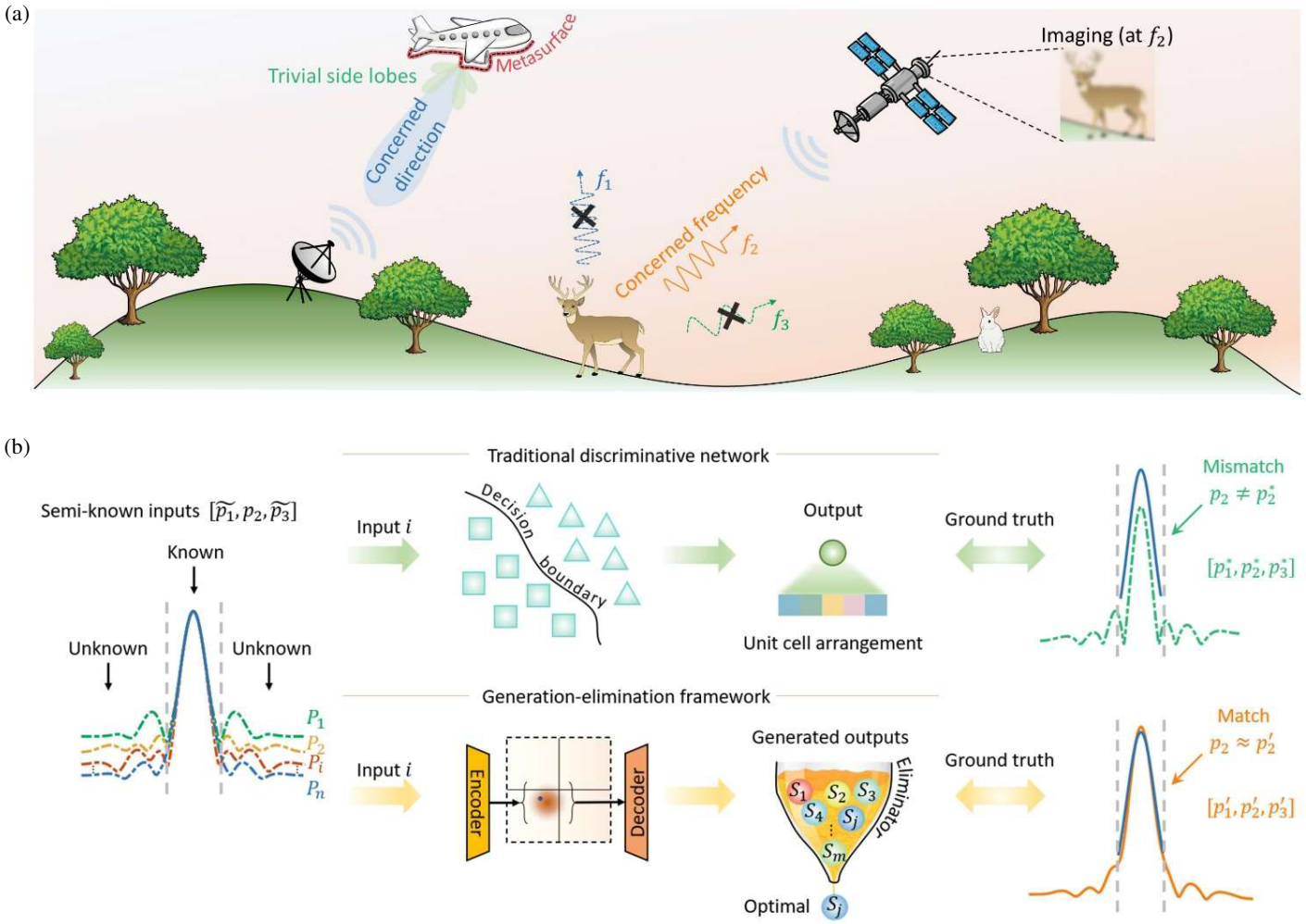

FIGURE 1. Schematic of intelligent metasurfaces with semi-known input. (a) Illustrative scenarios with semi-known input. (b) Comparison between traditional discriminative network and the proposed generation-elimination framework.

rect it? Similar examples are many in practice, but all of which remain unexplored. In this spirit, how to comprehensively cope with these situations with semi-known and noisy input is an important topic, albeit challenging.

To mitigate the challenge, we introduce a generation-elimination framework to facilitate metasurface design within complete and noisy input. The generation-elimination framework is composed of a conditional variational auto-encoder (CVAE) [28, 29] that automatically generates a diverse set of candidates and a forward prediction network (FPN) that filters inferior candidates. In this way, given a semi-known input, the generation-elimination framework can robustly distill the best output candidate. We verify the feasibility by two proof-of-the-concept cases, the on-demand metasurface design of the reflection spectra and the far-field pattern. The results show that, in the first case, the resonant frequency shift is less than 0.03 GHz, and in the second case, the mean absolute percentage error (MAPE) is less than 7% for the main lobe. In the experiment, we fabricated reconfigurable microwave metasurfaces to demonstrate the automatic beam steering used in vague wireless communication scene. Our work exhibits a promising approach to bring intelligent metasurfaces into a plethora of real-world applications incorporated with semi-known input and noisy information.

2. RESULTS

Illustrative applications of semi-known input in intelligent metasurfaces. The inverse design of intelligent metasurfaces means the direct retrieval of the proper metasurface structure and spatial distribution (output) for a user-desired electromagnetic response (input). However, in many cases, we only care about part of the input information while ignoring what happens in the rest. Real-world scenes with semi-known input are illustrated in Fig. 1(a). For example, for an airplane covered by the metasurfaces, we only need to steer the main lobe of scattering field towards the radar direction (deterministic part), without the requirement on side lobes (non-deterministic part). In addition, to image a deer, sometimes, we only care about the reflection spectra at certain frequencies, while ignoring the performance at other frequencies. For simplicity, we call this deterministic part as region of interest (ROI). The inputs that

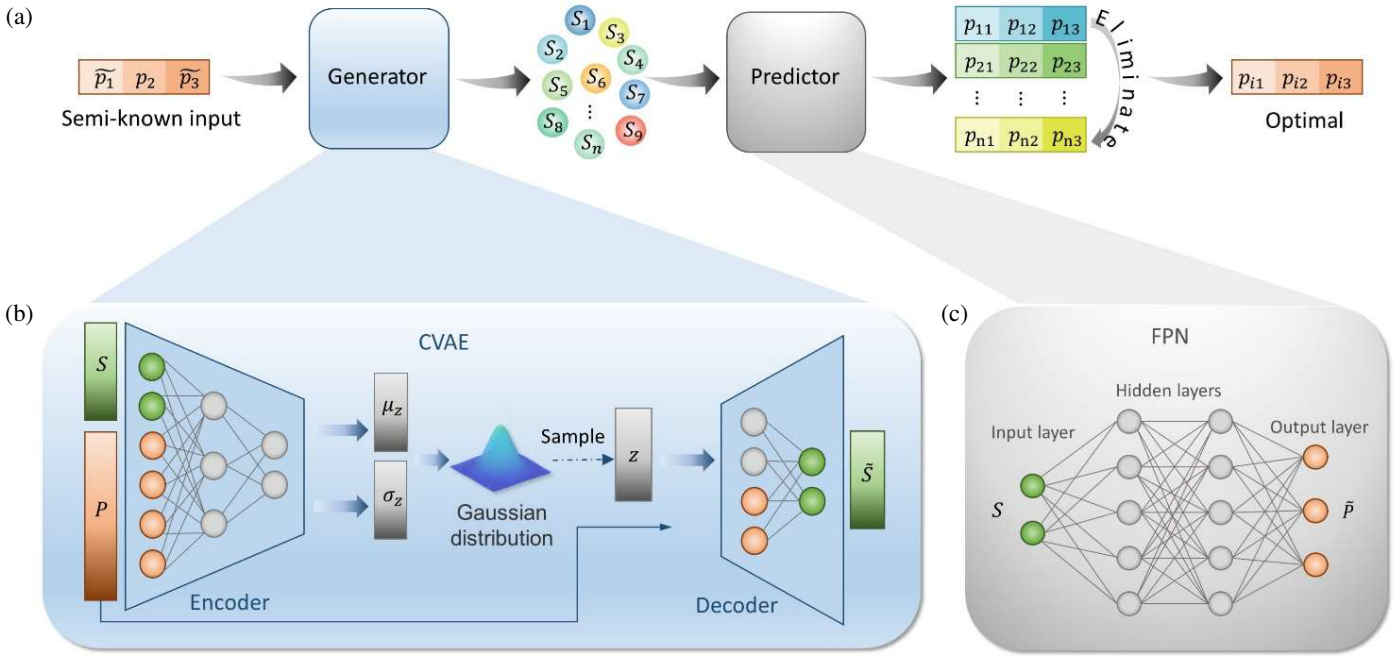

FIGURE 2. Architecture of the generation-elimination network. (a) The network comprises a generator and a predictor. Here, $P = \{\widetilde{p_1}, p_2, \widetilde{p_3}\}$ represents the electromagnetic response of metasurfaces, and S represents the geometries of unit cell or the distribution of metasurfaces. (b) The generator is a deep generative network, such as CVAE, to automatically generate a diverse set of metasurface candidates. (c) The predictor is a basic FPN to complete the mapping from the metasurfaces to the electromagnetic response.

satisfy the above ROI requirements are numerous, but each of which will make conventional neural network generate a completely different output. These outputs are either good or bad (depending on the repaired input version), but at least, they are not the optimal. Thus, it naturally raises the question of how to set up a suitable and complete input for the neural network to enable a robust and optimal result.

We formulate the above process in Fig. 1(b). In general, a semi-known input is expressed as $P = \{\widetilde{p_1}, p_2, \widetilde{p_3}\}$, where the middle interval p_2 is deterministic, and the other two, $\widetilde{p_1}$ and $\widetilde{p_3}$, are non-deterministic. It is infeasible to feed an incomplete input into conventional neural network, so that one has to artificially remedy the non-deterministic part. Correspondingly, conventional neural network gives a single output S^* (metasurface structure or distribution) that is very sensitive to the repaired version. Such S^* has the authentic electromagnetic response $P^* = \{p_1^*, p_2^*, p_3^*\}$ that may be distinct from the ground truth P, indicting that the inverse design result is terrible. To address this issue, we propose a generation-elimination architecture. We feed $P(\widetilde{p_1}$ and $\widetilde{p_3}$ are arbitrary) into the architecture that can generate a great number of candidates and eliminate all unsuitable candidates to retain the best candidate with $P' = \{p_1', p_2', p_3'\}$. It is very likely to make p_2' match well with p_2. Although p_1' and p_3' may be different from or consistent with $\widetilde{p_1}$ and $\widetilde{p_3}$, it is less important. Compared with conventional neural network, this architecture is more robust and can still generate a superior output even in the case of kaleidoscopic inputs.

Generation-elimination framework. The architecture of the whole network is depicted in Fig. 2(a), mainly composed of a generator and a predictor. The generator is a CVAE-based model that builds up a probabilistic relationship among variables and can automatically generate a family of nominated metasurface designs. The FPN-based predictor, acting as an inspector, is aimed for eliminating inferior candidates. As shown in Fig. 2(b), there are four types of variables in the framework: input variable S, condition variable P, output variable $\tilde{S}$, and latent variable z. The CVAE is proposed here to overcome the one-to-many issue that widely exists in the inverse design, because it can produce much more diverse candidates. The key point is that the true posterior distribution of the latent variable z that is conditioned on S and P, $p_\theta(z|x, y)$, is approximated by the approximate posterior $q_\varphi(z|x, y)$ and trained to be close to the prior probability $p_\theta(z) \sim \mathcal{N}(0, I)$, where φ is the variational parameter. Since we have applied a standard Gaussian prior distribution, φ_i would be (μ_i, σ_i). After training, any latent variable sampled from the $\mathcal{N}(0, I)$ would be interpreted as a new candidate once decoded. Thus, our CVAE-based generator is a deep generative model that can generate new structures containing similar features to those in the training data in a probabilistic manner. The CVAE is recognized for computational efficiency, particularly in handling high-dimensional data. By learning to generate representations in a lower-dimensional latent space conditioned on certain inputs, CVAEs reduce the computational burden significantly compared to traditional fully connected networks. Consequently, for tasks requiring the modeling of complex distributions or the generation of new samples conditional on specific inputs, CVAEs are generally more efficient and effective.

In the framework training process, the initial step involves training the FPN, illustrated in Fig. 2(c). This network is trained using the input S and the condition variable P. Then, we fix the

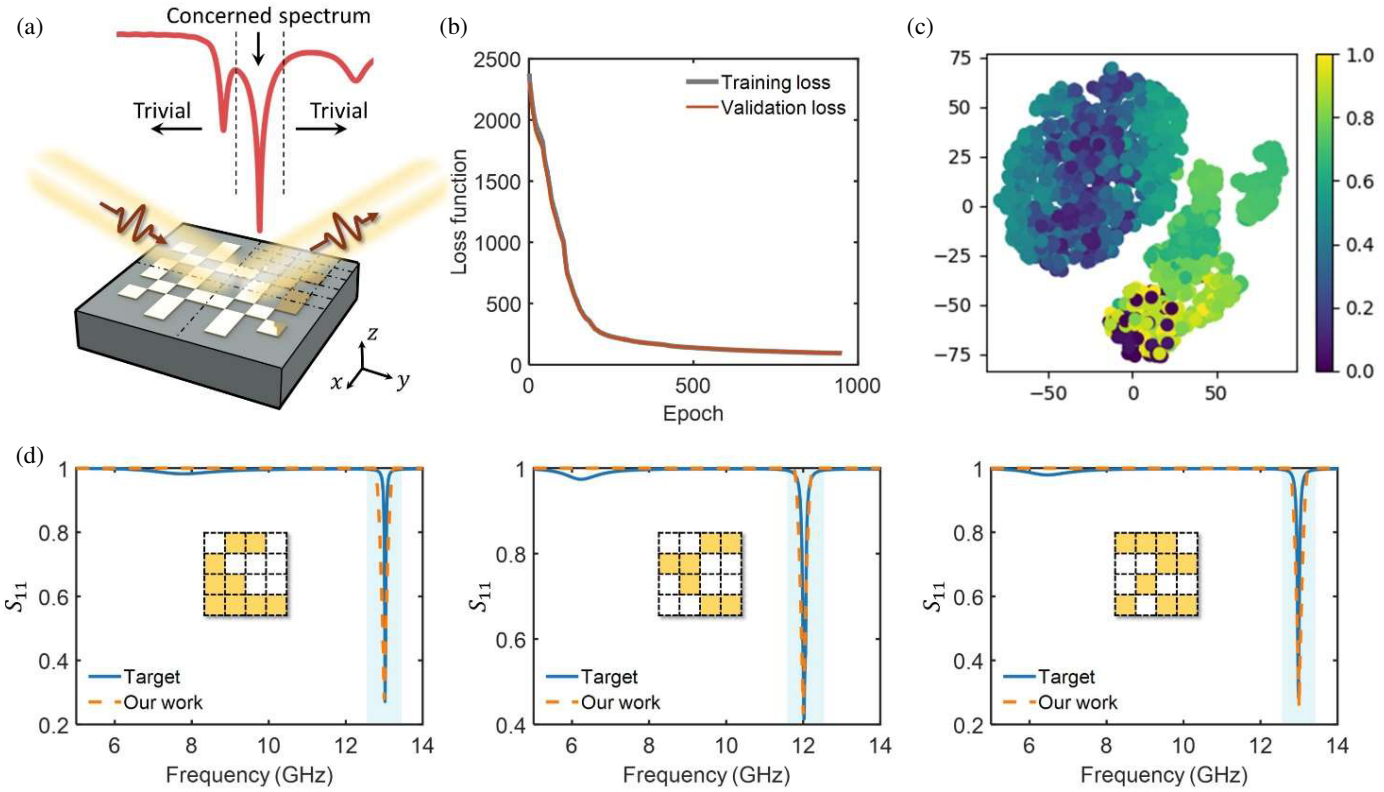

FIGURE 3. Demonstration in the inverse metasurface design with semi-known reflection coefficient. (a) Three-dimensional illustration of the metasurface. We consider a symmetrical metasurface structure, and discretize the upper metallic patch as a 5×5 matrix with the pixel size of 1.0 mm. By randomly setting the metallic patch, we can generate a great number of metasurfaces and obtain the reflection coefficient via numerical simulation. (b) The loss of the CVAE over epoch. (c) Latent space. In this space, each point represents a possible configuration of the underlying data. Similar data points are located closed to each other in the latent space, while dissimilar points are further apart. (d) Test instances.

parameters of the pre-trained FPN and connect it to the generator. The loss of the whole network comprises three parts, the reconstruction loss of S (calculated as the negative maximum likelihood), the Kullback-Leibler divergence that encourages a standard Gaussian distribution of z, and the mean squared error (MSE) of P and $\tilde{P}$. After training, the decoder of the generator is taken out to produce desired candidates. By feeding a semi-known input, we will obtain various sets of nominations, from which we can select the optimal one where the p_2 part is in good agreement with the final output.

Scenario 1: Inverse metasurface structural design with semi-known reflection coefficient. The first example we consider here is the inverse structural design of microwave metasurfaces. The basic unit cell/meta-atom is illustrated in Fig. 3(a), where the metallic patch is characterized by 0–1 matrix **R**; "1" signifies copper and "0" signifies vacuum. The spacing substrate is a commercial dielectric substrate with the dielectric constant $\varepsilon_r = 4.3$, loss tangent $\tan\delta = 0.0025$, and thickness $h = 2.0$ mm. The symmetrical metasurface has a period of 10 mm, thus described by 5×5 matrix. To reduce the mutual coupling among adjacent meta-atoms, we set a spacing of 1.0 mm between the boundary of the metallic pattern and the margin of the meta-atom. For the input variable S, the matrix is unfolded into a vector with 16 dimensions. For the semi-known input P, we take the reflection coefficient of the metasurface, i.e., the amplitude of S_{11} parameter. We want to note that a majority of previous studies consider the amplitude and phase of the reflection coefficient as the output format. However, since multiple abrupt wiggles exist at the resonant frequencies, using the amplitude and phase as the output format poses a significant challenge for the neural network to grasp the intricate relationship with trip points [25]. Therefore, we consider the resonant frequency, amplitude, and bandwidth as the input condition, where the whole spectrum ranges from 5 to 15 GHz.

The FPN is composed of 8 hidden layers with 1,000 neurons per layer. The activation function chosen for the hidden layers is the Rectified Linear Unit (ReLU), while the Sigmoid function is selected as the activation function for the last layer to ensure that the final responses are within the range of (0, 1). After the FPN has been established, the next step is to train the CVAE. In above process, a total number of 10,900 samples are used for training, split into training, validation, and test set with 80%, 10%, and 10% ratio. The samples are obtained by co-simulation performed using the commercial software CST Microwave Studio and MATLAB. As shown in Fig. 3(c), the latent space of a CVAE is a 2-dimensional vector space in which each point represents a possible configuration of the underlying data. Similar data points are located closed to each other in the latent space, while dissimilar points are further apart. By exploring and manipulating the latent space, new data points

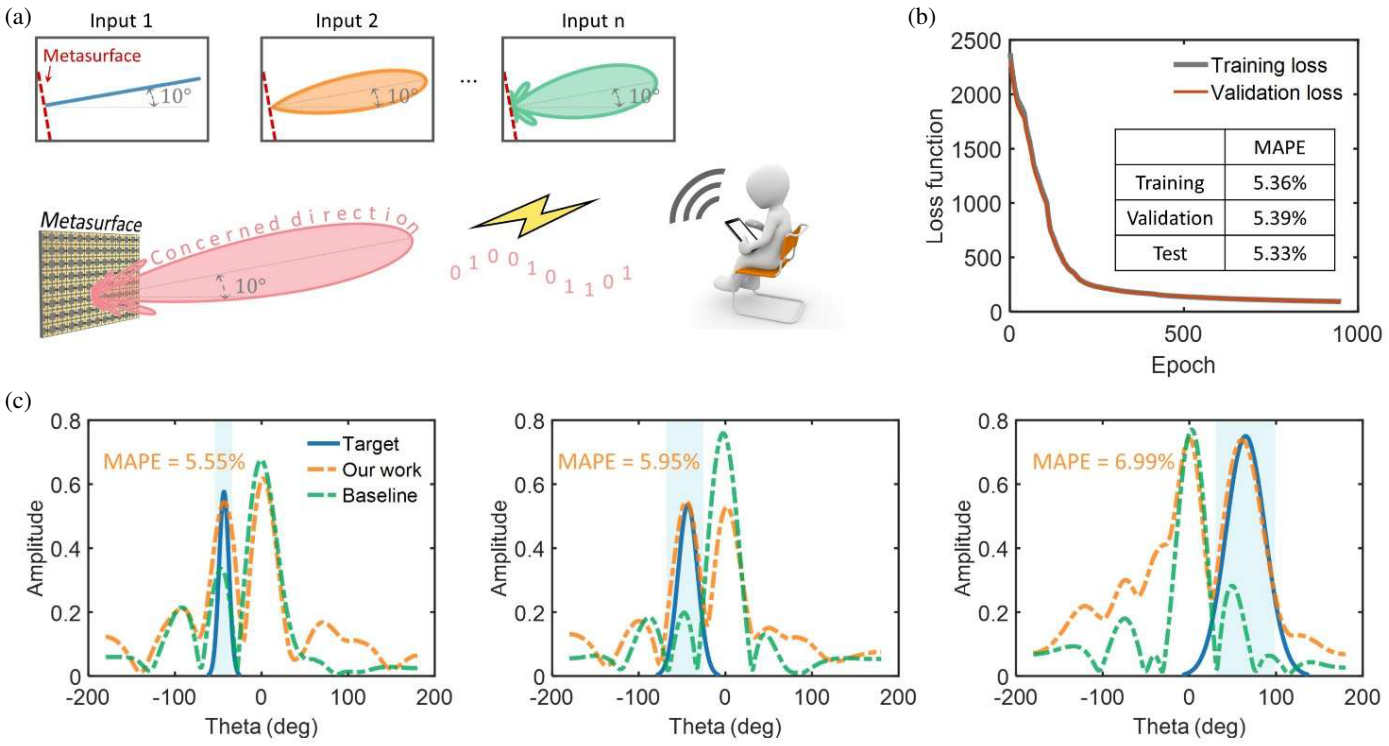

FIGURE 4. Demonstration in the inverse metasurface design with semiknown far-field pattern. (a) In communication scene, to steer the main lobe towards the user's direction, the inputs are many, having different width at half maxima and side lobes. For those inputs, the generated outputs are different. The perfect input field is a delta function (input 1). Yet, it does not mean that the generated output will be the best. Moreover, delta output is almost impossible to be reached in practice. (b) The loss of the CVAE over epoch. (c) Test instances. The light blue region denotes the region of interest. Baseline means conventional discriminative neural network, i.e., a fully connected neural network.

can be generated and the relationships between different data points can be analyzed. The performance of the network can be seen in Fig. 3(b), and the specific testing results are presented in Fig. 3(d). With the input resonant frequencies of 13.024 GHz, 12.023 GHz, and 12.985 GHz, the network produces the outputs of 12.998 GHz, 11.997 GHz, and 12.998 GHz, respectively, with an error of less than 0.03 GHz. The desired reflection coefficients are 0.2712, 0.4127, and 0.2842, consistent with the reflection coefficients generated by the network, 0.2857, 0.4344, and 0.2638.

Scenario 2: far-field customization of metasurfaces. The proposed method can also be employed in the global far-field customization. In the fifth generation (5G) wireless communication scenario, the demand for real-time localization and tracking services becomes increasingly urgent. In the past decade, intelligent metasurfaces have found to be a superior candidate for manipulating wireless channels in a green and cost-effective manner. However, how to construct a suitable input of real-world scenario for intelligent metasurfaces is the core. For instance, to steer the main lobe towards a direction, the perfect input field is a delta function (the inset of Fig. 4(a)). Yet, it is almost impossible to be reached in practice. Even though we feed the delta function into the pre-trained neural network, it does not mean that the output field is also the optimal one. One may conceive the input field with different widths at half maxima and side lobes, as long as the main lobe is directed towards the defined direction. In this vein, we can easily find that this is a semi-known problem, having infinite possibilities.

As a demonstration, we posit that the metasurface is composed of 8×32 identical unit cells and that the far-field distribution is calculated based on antenna theory; the size of unit cell is $7.5 \times 7.5\,\text{mm}^2$. In this case, the semi-known input P is far-field pattern, and the input variable S is the phase of the unit cell. An FPN consisting of 8 hidden layers and 1,000 neurons per layer was selected, with a rectified linear unit (ReLU) used as the activation function for the hidden layers. The next step is to train the CVAE with the FPN connected behind. We trained the FPN and CVAE using 100,000 samples at 7.0 GHz. The network performance is shown in Fig. 4(c), and the test results are shown in Fig. 4(b). To intuitively exhibit the results, we randomly produce the known part, and the unknown part is artificially constructed. It turns out that the CVAE can generate results with the MAPE of only 5.55%, 5.95% and 6.99%, compared to 39.42%, 63.82%, and 73.41% for traditional neural network. The results reveal that the CVAE output is remarkably robust, generating high-quality results irrespective of the main lobe width or the shape of its side lobes.

Experiment verification. To demonstrate the real-world significance in wireless communications, we fabricated the reconfigurable metasurfaces in a microwave experiment on the

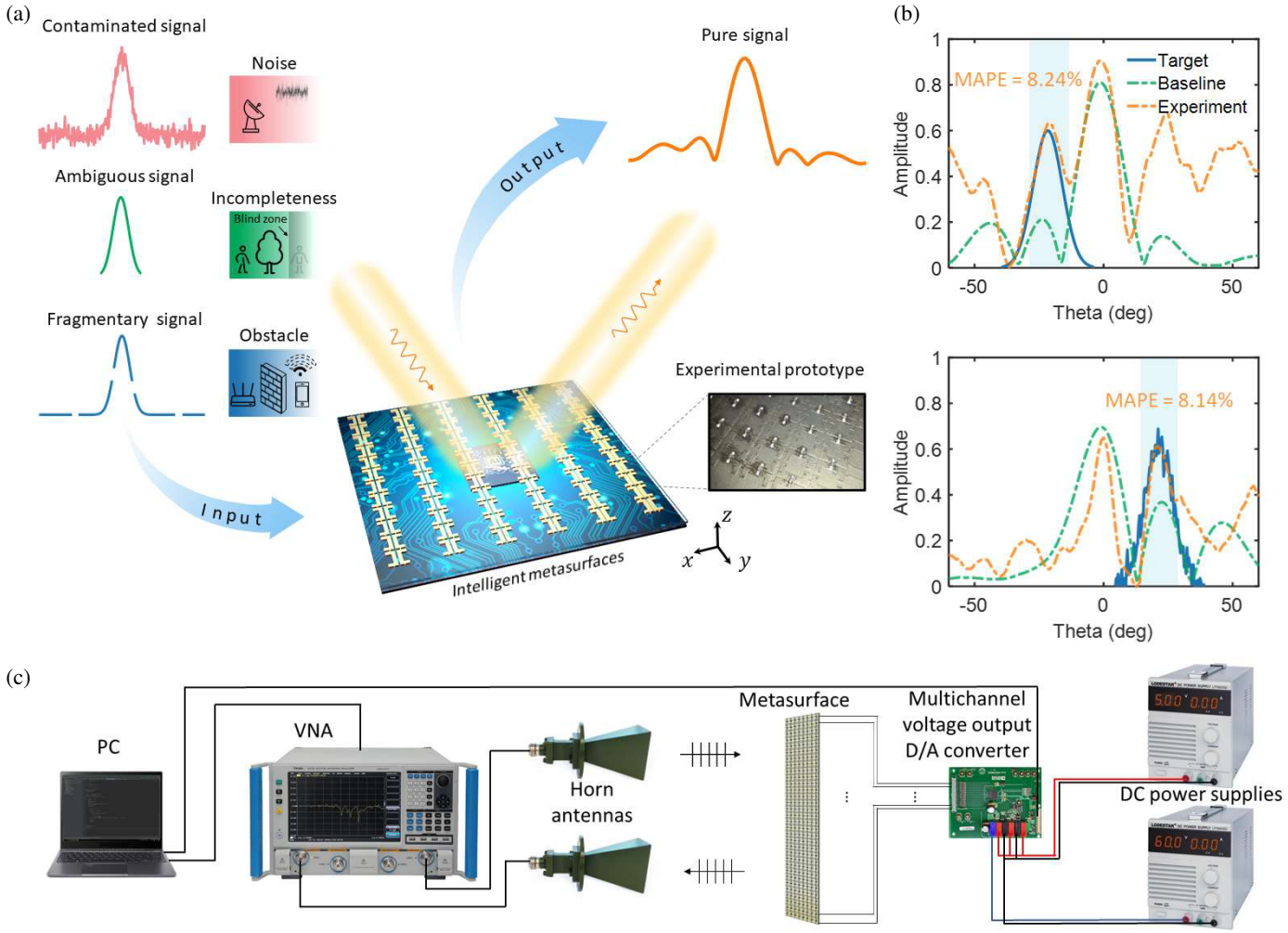

FIGURE 5. Experimental verification of the generation-elimination framework enabled intelligent metasurfaces for semi-known input. (a) Application scenarios of the generation-elimination framework. (b) Experimental results. The light blue region denotes the region of known far-field. Baseline means conventional discriminative neural network, i.e., a fully connected neural network. (c) Experimental setup connection diagram.

basis of Scenario 2. As shown in Fig. 5(a), the real-world signal that is input to the neural network may be contaminated, ambiguous, and fragmentary. Intelligent metasurfaces aim to convert these inputs into practical realization. For these undesired and disturbed cases, intelligent metasurfaces are robust to generate high-quality scattering field only based on the interested part. The lower right corner shows the experimental prototype of reconfigurable metasurfaces, each of which is incorporated with active components.

The basic reconfigurable metasurface is illustrated in Fig. 5(c). We selected an F4B substrate with a dielectric constant of 3.5 and a loss tangent of 0.003 for our study. The metasurface inclusion has dimensions of $90 \times 250 \times 2\,\text{mm}^3$ (8×32 unit cells). In the y-direction, every column (8 unit cells) shares the same bias voltage, with varactor diodes attached between the metallic split I-shaped islands on the dielectric substrate. As a result, we only need to consider 32 bias voltages for the entire metasurface inclusion. We used the SMV2019-079LF varactor diode from Skyworks Solutions, Inc. for the metasurface. To dynamically tune the reflection spectrum, a reverse bias voltage ranging from 0 to 20 V was applied to each unit cell to control the capacitance of the varactor diode.

The experimental setup is illustrated in Fig. 5(c). The semi-known input P is a far-field pattern, and the input variable S is the bias voltage of the meta-atom. We feed different bias voltage across the varactor diode and measure the voltage-phase correspondence to be ready for network training. We measure the far-field directional map of the metasurface by placing it on a rotating platform and receiving the signal through a horn antenna connected to a vector network analyzer. Experimental results are shown in Fig. 5(b). For the artificially-constructed inputs, the MAPE between the target responses and experimental results on the main lobe is 8.24% and 8.14%, respectively. This is in stark contrast to traditional neural network, which exhibits 37.51% and 70.24% for the same inputs. The proof-of-concept cases and experimental results presented above demonstrate the ability to generate high-quality output despite semi-known input. Additionally, the framework exhibits a remarkable level of robustness, further highlighting its potential in communica-

tion scenarios where inputs may be contaminated by noise and information incompleteness. Our generation-elimination network, while robust, exhibits a dependence on the availability of substantial volumes of high-quality training data to faithfully characterize the underlying data distribution. Future iterations of our research will prioritize the development of more efficient data acquisition methodologies to mitigate this limitation and enhance the network's applicability.

3. CONCLUSION

To sum up, we introduced a generation-elimination framework to enable intelligent metasurfaces toward semi-known and noisy input. This framework has improved the robustness over the conventional discriminative network and provides a superior output even in the presence of an input that is somewhat out of the ordinary. We have verified the idea by two cases, the on-demand metasurface design of the reflection coefficient and the far-field pattern. More prominently, the generation-elimination framework can be readily extended into other research domains of optics and materials science with semi-known input and information pollution, leading to a variety of photonic designs and a broad range of real-world applications, such as cloaking, imaging, and wireless communications [3, 5, 21, 26, 30–45]. In the foreseeable future, along with the influx of massive data, we have to encounter more and more data with unexpected noise, incomplete annotation, and information disclosure, making the application with semi-known input widely exist. We anticipate that the proposed framework may become a safe scaffolding to be relied on and promise the access to a full-featured intelligent metasurfaces.

ACKNOWLEDGEMENT

This work at Zhejiang University was sponsored by the National Natural Science Foundation of China (NNSFC) under Grant Nos. 61625502, 11961141010, 61975176, 62071424, and 62101485, Young Elite Scientists Sponsorship Program by CAST (2022QNRC001), the Top-Notch Young Talents Program of China, and the Fundamental Research Funds for the Central Universities.

Methods

Data collection. The training data for Scenario 1 was obtained via co-simulation using the commercial software CST Microwave Studio and MATLAB. Initially, MATLAB generates the pattern matrix **R** by uniformly sampling the complete solution space and converting it into the corresponding binary matrix. Subsequently, the actual metasurfaces are imported into CST Microwave Studio to calculate the reflection coefficient. The reflection spectra of interestare set within the microwave region from 5 to 15 GHz, discretized into 1,001 data points at uniform interval. The frequency, amplitude, and bandwidth of the resonance point are calculated from the amplitude data. For Scenario 2, MATLAB is used to generate the training data based on antenna theory.

Experimental setup. The metasurface is mounted on a rotating platform that is controlled by a PC through a serial port. Two DC-regulated power supplies, LODESTAR LPS605D, connected to a multichannel voltage output D/A converter, the AD5535B, are used to supply power to the metasurface. The voltage output channels of the converter are controlled through a computer program, with 32 channels connected to the 32 columns of the metasurface correspondingly, and the voltages are set based on the results generated by the network. The signal is received via two horn antennas connected to a vector network analyzer, the Ceyear 3672C, and the PC can read the VNA data through a network cable.

Author contributions

C.Q., P.L., and H.C. conceived the idea of this research. P. L. performed modelling of the network and data analysis. J.Z., J.C., and X.Z. assisted in machine learning. P.L. and C.Q. wrote the paper. All authors contributed to discussions on the results. C.Q. and H.C. supervised the project.

Data availability

The data that support the findings of this study are available from the authors on reasonable request.

Competing interests

The authors declare no competing financial interests.

REFERENCES

[1] Liu, D., Y. Li, J. Lin, H. Li, and F. Wu, "Deep learning-based video coding: A review and a case study," *ACM Computing Surveys*, Vol. 53, No. 1, 1–35, Feb. 2020.

[2] Wang, Z., J. Chen, and S. C. H. Hoi, "Deep learning for image super-resolution: A survey," *IEEE Transactions on Pattern Analysis and Machine Intelligence*, Vol. 43, No. 10, 3365–3387, Oct. 2021.

[3] Purwins, H., B. Li, T. Virtanen, J. Schlueter, S.-Y. Chang, and T. Sainath, "Deep learning for audio signal processing," *IEEE Journal of Selected Topics in Signal Processing*, Vol. 13, No. 2, 206–219, May 2019.

[4] Qian, C., Y. Yang, Y. Hua, C. Wang, X. Lin, T. Cai, D. Ye, E. Li, I. Kaminer, and H. Chen, "Breaking the fundamental scattering limit with gain metasurfaces," *Nature Communications*, Vol. 13, No. 1, 4383, Jul. 2022.

[5] Cai, T., B. Zheng, J. Lou, L. Shen, Y. Yang, S. Tang, E. Li, C. Qian, and H. Chen, "Experimental realization of a superdispersion-enabled ultrabroadband terahertz cloak," *Advanced Materials*, Vol. 34, No. 47, 2205053, Nov. 2022.

[6] Jia, Y., C. Qian, Z. Fan, T. Cai, E.-P. Li, and H. Chen, "A knowledge-inherited learning for intelligent metasurface design and assembly," *Light Science & Applications*, Vol. 12, No. 1, 82, Mar. 2023.

[7] He, Q., S. Sun, and L. Zhou, "Tunable/Reconfigurable metasurfaces: Physics and applications," *Research*, Vol. 2019, 1849272, 2019.

[8] Huang, C., C. Zhang, J. Yang, B. Sun, B. Zhao, and X. Luo, "Reconfigurable metasurface for multifunctional control of electromagnetic waves," *Advanced Optical Materials*, Vol. 5, No. 22, 1700485, Nov. 2017.

[9] Chen, J., C. Qian, J. Zhang, Y. Jia, and H. Chen, "Correlating metasurface spectra with a generation-elimination framework," *Nature Communications*, Vol. 14, No. 1, 4872, Aug. 2023.

[10] Wang, Z., M. Chen, C. Qian, Z. Fan, H. Wang, and H. Chen, "Reconfigurable matrix multiplier with on-site reinforcement learning," *Optics Letters*, Vol. 47, No. 22, 5897–5900, Nov. 2022.

[11] Zhang, J., C. Qian, J. Chen, B. Wu, and H. Chen, "Uncertainty qualification for metasurface design with amendatory Bayesian network," *Laser & Photonics Reviews*, Vol. 17, No. 5, 2200807, May 2023.

[12] Khatib, O., S. Ren, J. Malof, and W. J. Padilla, "Deep learning the electromagnetic properties of metamaterials — A comprehensive review," *Advanced Functional Materials*, Vol. 31, 2101748, Aug. 2021.

[13] Ramprasad, R., R. Batra, G. Pilania, A. Mannodi-Kanakkithodi, and C. Kim, "Machine learning in materials informatics: Recent applications and prospects," *NPJ Computational Materials*, Vol. 3, 54, Dec. 2017.

[14] Jia, Y., C. Qian, Z. Fan, Y. Ding, Z. Wang, D. Wang, E.-P. Li, B. Zheng, T. Cai, and H. Chen, "In situ customized illusion enabled by global metasurface reconstruction," *Advanced Functional Materials*, Vol. 32, No. 19, 2109331, May 2022.

[15] Fan, Z. and et al., "Transfer-learning-assisted inverse metasurface design with 30% data savings," *Phys. Rev. Appl.*, Vol. 18, 024022, 2022.

[16] Fan, Z., C. Qian, Y. Jia, Z. Wang, Y. Ding, D. Wang, L. Tian, E. Li, T. Cai, B. Zheng, I. Kaminer, and H. Chen, "Homeostatic neuro-metasurfaces for dynamic wireless channel management," *Science Advances*, Vol. 8, No. 27, eabn7905, Jul. 2022.

[17] Gao, L., X. Li, D. Liu, L. Wang, and Z. Yu, "A bidirectional deep neural network for accurate silicon color design," *Advanced Materials*, Vol. 31, No. 51, 1905467, Dec. 2019.

[18] Qian, C., Z. Wang, H. Qian, T. Cai, B. Zheng, X. Lin, Y. Shen, I. Kaminer, E. Li, and H. Chen, "Dynamic recognition and mirage using neuro-metamaterials," *Nature Communications*, Vol. 13, No. 1, 2694, May 2022.

[19] Jiang, J. and J. A. Fan, "Global optimization of dielectric metasurfaces using a physics-driven neural network," *Nano Letters*, Vol. 19, No. 8, 5366–5372, Aug. 2019.

[20] Wiecha, P. R. and O. L. Muskens, "Deep learning meets nanophotonics: A generalized accurate predictor for near fields and far fields of arbitrary 3D nanostructures," *Nano Letters*, Vol. 20, No. 1, 329–338, Jan. 2020.

[21] Qian, C., B. Zheng, Y. Shen, L. Jing, E. Li, L. Shen, and H. Chen, "Deep-learning-enabled self-adaptive microwave cloak without human intervention," *Nature Photonics*, Vol. 14, No. 6, 383, Jun. 2020.

[22] Wang, Z., C. Qian, T. Cai, L. Tian, Z. Fan, J. Liu, Y. Shen, L. Jing, J. Jin, E.-P. Li, B. Zheng, and H. Chen, "Demonstration of spider-eyes-like intelligent antennas for dynamically perceiving incoming waves," *Advanced Intelligent Systems*, Vol. 3, No. 9, 2100066, Sep. 2021.

[23] Raccuglia, P., K. C. Elbert, P. D. F. Adler, C. Falk, M. B. Wenny, A. Mollo, M. Zeller, S. A. Friedler, J. Schrier, and A. J. Norquist, "Machine-learning-assisted materials discovery using failed experiments," *Nature*, Vol. 533, No. 7601, 73–76, May 2016.

[24] Qian, C., X. Lin, X. Lin, J. Xu, Y. Sun, E. Li, B. Zhang, and H. Chen, "Performing optical logic operations by a diffractive neural network," *Light Science & Applications*, Vol. 9, No. 1, 59, Apr. 2020.

[25] Zhang, J., C. Qian, Z. Fan, J. Chen, E. Li, J. Jin, and H. Chen, "Heterogeneous transfer-learning-enabled diverse metasurface design," *Advanced Optical Materials*, Vol. 10, No. 17, 2200748, Sep. 2022.

[26] Wu, N., Y. Jia, C. Qian, and H. Chen, "Pushing the limits of metasurface cloak using global inverse design," *Advanced Optical Materials*, Vol. 11, No. 7, 2202130, Apr. 2023.

[27] Zhu, X., C. Qian, Y. Jia, J. Chen, Y. Fang, Z. Fan, J. Zhang, D. Li, R. Abdi-Ghaleh, and H. Chen, "Realization of index modulation with intelligent spatiotemporal metasurfaces," *Advanced Intelligent Systems*, Vol. 5, No. 7, 2300065, Jul. 2023.

[28] Kingma, D. P. and M. Welling, "Auto-encoding variational bayes," http://arxiv.org/abs/1312.6114, 2014.

[29] Sohn, K., X. Yan, and H. Lee, "Learning structured output representation using deep conditional generative models," in *Advances in Neural Information Processing Systems (NIPS 2015)*, Vol. 28, Dec. 2015.

[30] Qian, C. and H. Chen, "A perspective on the next generation of invisibility cloaks-intelligent cloaks," *Applied Physics Letters*, Vol. 118, No. 18, 180501, May 2021.

[31] Zhen, Z., C. Qian, Y. Jia, Z. Fan, R. Hao, T. Cai, B. Zheng, H. Chen, and E. Li, "Realizing transmitted metasurface cloak by a tandem neural network," *Photonics Research*, Vol. 9, No. 5, B229–B235, May 2021.

[32] Wu, Q. and R. Zhang, "Intelligent reflecting surface enhanced wireless network via joint active and passive beamforming," *IEEE Trans. Wireless Commun.*, Vol. 18, 5394–5409, 2019.

[33] Basar, E., "Reconfigurable intelligent surface-based index modulation: A new beyond MIMO paradigm for 6G," *IEEE Transactions on Communications*, Vol. 68, No. 5, 3187–3196, May 2020.

[34] Hu, Q. and et al., "An intelligent programmable omni-metasurface," *Laser Photon. Rev.*, Vol. 16, 2100718, 2022.

[35] Lu, H., J. Zhao, B. Zheng, C. Qian, T. Cai, E. Li, and H. Chen, "Eye accommodation-inspired neuro-metasurface focusing," *Nature Communications*, Vol. 14, No. 1, 2023.

[36] Zhang, K. and et al., "Ultrasensitive self-driven terahertz photodetectors based on low-energy type-II dirac fermions and related van der Waals heterojunctions," *Small*, Vol. 19, 2205329, 2023.

[37] Hu, Z. and et al., "Terahertz nonlinear hall rectifiers based on spin-polarized topological electronic states in 1T-CoTe2," *Advanced Materials*, Vol. 35, 2209557, 2023.

[38] Rizza, C., D. Dutta, B. Ghosh, F. Alessandro, C.-N. Kuo, C. S. Lue, L. S. Caputi, A. Bansil, V. Galdi, A. Agarwal, A. Politano, and A. Cupolillo, "Extreme optical anisotropy in the type-II dirac semimetal NiTe2 for applications to nanophotonics," *ACS Applied Nano Materials*, Vol. 5, No. 12, 18 531–18 536, Dec. 2022.

[39] Daws, S., P. Kotak, C.-N. Kuo, C. S. Lue, A. Politano, and C. Lamuta, "Platinum diselenide PtSe2: An ambient-stable material for flexible electronics," *Materials Science and Engineering B-Advanced Functional Solid-State Materials*, Vol. 283, 115824, Sep. 2022.

[40] Vobornik, I., A. B. Sarkar, L. Zhang, D. W. Boukhvalov, B. Ghosh, L. Piliai, C.-N. Kuo, D. Mondal, J. Fujii, C. S. Lue, M. Vorokhta, H. Xing, L. Wang, A. Agarwal, and A. Politano, "Kitkaite nitese, an ambient-stable layered dirac semimetal with low-energy type-II fermions with application capabilities in spintronics and optoelectronics," *Advanced Functional Materials*, Vol. 31, No. 52, 2106101, Dec. 2021.

[41] Faenzi, M. and et al., "Metasurface antennas: New models, applications and realizations," *Sci. Rep.*, Vol. 9, 10178, 2019.

[42] Badawe, M. E., T. S. Almoneef, and O. M. Ramahi, "A true metasurface antenna," *Sci. Rep.*, Vol. 6, 19268, 2016.

[43] Tan, Q., C. Qian, T. Cai, B. Zheng, and H. Chen, "Solving multivariable equations with tandem metamaterial kernels," *Progress*

In Electromagnetics Research, Vol. 175, 139–147, 2022.

[44] Shou, Y., Y. Feng, Y. Zhang, H. Chen, and H. Qian, "Deep learning approach based optical edge detection using ENZ layers," *Progress In Electromagnetics Research*, Vol. 175, 81–89, 2022.

[45] Xie, H., T. Hu, Z. Wang, Y. Yang, X. Hu, W. Qi, and H. Liu, "A physics-based HIE-FDTD method for electromagnetic modeling of multi-band frequency selective surface," *Progress In Electromagnetics Research*, Vol. 173, 129–140, 2022.